
Wesleyan University

A Clever Title

by

Jonas Powell
Class of 2019

A thesis submitted to the
faculty of Wesleyan University
in partial fulfillment of the requirements for the
Degree of Master of Arts

Middletown, Connecticut

April, 2018

*If people sat outside and looked at the stars each night,
I'll bet they'd live a lot differently.*

—CALVIN & HOBBES

Contents

1	Introduction	1
1.1	Submillimeter Observations	4
1.1.1	Interferometry	5
1.1.2	Continuum Emission	12
1.1.3	Line Emission	13
1.2	Disk & The Role of Environment	16
1.2.1	The Minimum Mass Solar Nebula	16
1.2.2	Low- and High-Mass Star Forming Regions	17
1.3	d253-1536: A Misaligned Binary System	21
1.3.1	Local Environment & Features	21
1.3.2	Previous Observations	23
1.4	Summary of Contents	25
	Bibliography	26

List of Figures

1.1	An edge-on slice of a protoplanetary disk is presented (Dullemond & Monnier, 2010 reference). As is visible in this graphic, significant radial segmentation of the disk exists, particularly between the inner gas disk and outer disk of gas, dust, and planetesimals. Also of note is the large vertical flaring that occurs at large radii. Since the observations that this thesis are based on were made with ALMA, we are sensitive primarily to the outer reaches of the disk.	3
1.2	Two example SEDs, accompanied by cartoon models to illustrate the various contributions of different elements of a disk and their influences on the SED. The dashed line corresponds to emission from the stellar photosphere, while the colored lines are blackbody curves corresponding to emission from the similarly-colored ring in the cartoon disk below each SED. Curves that peak at shorter wavelengths come from hotter dust. REWORK	6
1.4	Left: A rendering of ALMA (reference) shows the interferometer's antennae in the high desert, as well as a purpose-built truck moving one of the antennae (lower right). Right: A recent survey from ALMA reveals stunning detail in several protoplanetary disks. Andrews et al 2018 reference	12

1.5 An example of a moment-one map of a protoplanetary disk that is seen approximately edge-on, drawn from de Gregorio-Monsalvo et al 2013 reference. Colors correspond to intensity-weighted velocity; in other words, how quickly material is moving relative to the observer. This image immediately offers us several pieces of information: for example, the disk's northeast side is moving away from us while the southwest side is coming towards us, and the disk as a whole is receding from us at around 6 km/s, which we know due to the fact that the material with zero disk velocity (in green) corresponds to a velocity of 6 km/s relative to us.	15
1.6 NASA press image of a selection of proplyds in the Orion Nebula. The closer a proplyd is to a large, bright star, the more visibly windswept it is. Image courtesy of HST	19
1.8 <i>Left:</i> The masses of 70 ONC proplyds are plotted against their projected distance from the Orion Nebula's central O-star, θ^1 Ori C, drawn from surveys from ALMA and the SMA (Mann et al 2014 reference). Grey markers indicate 3σ upper limits for non-detections. The dashed line at $10 M_{Jup}$ indicates the minimum-mass solar nebula. As is clear from this plot, a statistically-significant correlation was found between disk mass and distance from θ^1 Ori C. <i>Right:</i> Radius is also affected by proximity to θ^1 Ori C (Eisner et al (2018) reference)	22

1.10 Images of V2434 Ori taken from Smith et al (2005 reference) on HST (Fig. 1.9a), Mann et al (2009 reference) with the SMA at 880 μ m (Fig. 1.9b), and Ricci et al (2011 reference) with the EVLA at 7mm (Fig. 1.9c). The ionization front is clearly visible in both the HST and EVLA observations, and the jet from disk A is visible in the HST image.	23
1.12 Moment-1 maps of HCO^+ , HCN, CO, and CS emission (left to right) in the present study's proplyds.	24

Chapter 1

Introduction

Planetary systems, including our own Solar System, are born from circumstellar disks of gas and dust around young stars. Young ($\leq 10\text{Myr}$) circumstellar disks, known as protoplanetary disks, are easily distinguishable from their older siblings by their large abundance of gas, which typically outweighs the disk's dust by a factor of 100. However, as these disks age they are influenced by gravitational, chemical, and viscous forces, and their gas almost entirely dissipates as they become debris disks, much like our familiar local Solar System's Kuiper Belt and asteroid belt. But while we can observe with relative ease the current state of our local planetary system and debris disks, understanding the process that brought us here is much more difficult. To do so, we must understand the nature of our own disk at its birth, and whether or not that process is a common one that we would expect to see replicated elsewhere. To understand this mystery, we must turn to observations of other comparable protoplanetary disks in order to develop a coherent narrative of disk evolution and, consequently, the conditions necessary for planet formation.

To understand the birth of our protoplanetary disk, we must understand the birth of our Sun, as the two are intimately related. Stars form when a region of a molecular cloud develops a gravitational instability sufficient to lead to a runaway collapse (reference). In this process, the cloud shrinks by a factor of around ten

million on its way down to a star, analogous to shrinking a square the approximate size of Connecticut ($\sim 150 \times 150$ km) down to just 15mm on each side, leading to a tremendous increase in rotational velocity in order to conserve angular momentum. As the local material begins to self-gravitate, its center forms a dense core which will eventually become a young star (binaries are also a common outcome in this process; according to Duchene & Kraus 2013 (reference), approximately half of all stars are found in binary systems).

However, if that angular momentum is conserved only through an increase in angular velocity, velocities will become so large that the star itself will be unable to form, as centrifugal forces pulling outward will become more significant than the gravitation pulling the star in on itself. In order to prevent velocities from becoming this high, stellar jets and disks, made from the collapsing material, will develop to decentralize the system's mass and dissipate its angular momentum.

The resulting disks present flared radial structures, typically extending several hundred AU (Vincente & Alves 05 reference). Since these disks form directly out of the collapse process, they, like their stellar host and the initial molecular cloud, are initially composed almost exclusively of molecular hydrogen, although their chemical evolution is significant and heavily studied. Temperatures in their outer reaches are typically in the 10-100 K range; masses range from ones to tens of Jovian masses (Andrews & Williams 05 reference), but this value comes with significant assumptions. Masses for the disks in the present study are calculated in Chapter ??.

By around 10 Myr, the primordial gas and dust in these disks is depleted by several processes, including accretion onto the host star, blowing out from radiation pressure, and becoming locked up in icy bodies, transitioning the disk from a protoplanetary disk to a debris disk. These new debris disks are made up

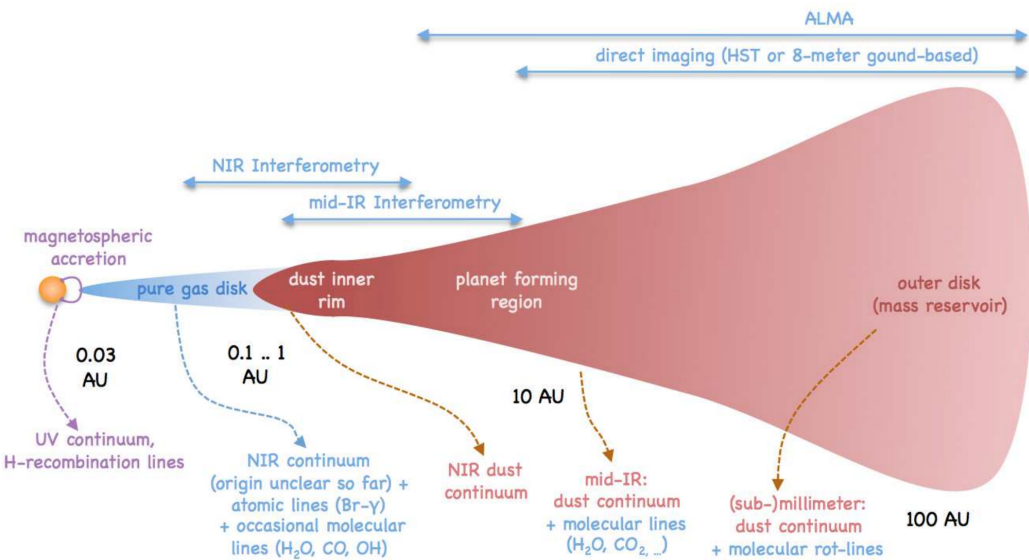


Figure 1.1: An edge-on slice of a protoplanetary disk is presented (Dullemond & Monnier, 2010 reference). As is visible in this graphic, significant radial segmentation of the disk exists, particularly between the inner gas disk and outer disk of gas, dust, and planetesimals. Also of note is the large vertical flaring that occurs at large radii. Since the observations that this thesis are based on were made with ALMA, we are sensitive primarily to the outer reaches of the disk.

of what is thought to be second generation dust, created by the grinding down of boulders and planetesimals, since any primordial dust from the initial collapse should have been blown out by this time. The gas masses in debris disks tend to be orders of magnitude lower than in protoplanetary disks. For a more complete review of disk evolution, see Hughes et al (2018).

1.1 Submillimeter Observations

Although protoplanetary disks' *relative* dust abundance is low, the actual amount of material that they harbor early in their lives is quite substantial (RELATIVE TO).

although ppds mass id dominated by gas, they still have sufficient dust to be optically thick in the optical. Therefore, we can't measure their mass at optical wavelengtsh and should use mm obs. REWORK

This makes it difficult to make measurements of dust mass in the optical, since at these wavelengths the dust is optically thick. However, since the optical depth of the dust at millimeter wavelengths is low, and since the emission being observed at these wavelengths is thermal rather than due to scattering (as it is in the optical), observations at millimeter wavelengths are preferred for measuring a disk's dust mass.

In the radio, we may trace two types of emission:

- CONTINUUM EMISSION: Although the size distribution of grain in a dust disk is wide and heavily weighted towards smaller grains, larger, millimeter-sized grains are still present in disks. These larger grains are far more efficient emitters in the radio, since the wavelength of a grain's peak thermal emission efficiency is approximately equal to its size. Thus, we may observe

this continuum emission (so named thanks to the wide range of frequencies that thermal emission covers) from these millimeter-sized grains.

- **LINE EMISSION:** Because radial disk temperatures quickly fall below the temperatures required to cause photodissociation, molecules may live a stable existence in these disks. Conveniently, the rotational transitions of small molecules tend to occur at energies in the millimeter wavelength regime. Observations of the emission from these rotational transitions, known as line emission, can provide us with a wealth of important information, including kinematics, temperature information, disk chemistry and total disk mass.

Notably absent in both forms is emission from the central star, thanks to the fact that stars are extremely weak emitters in the radio regime, since stars are hot and, consequently, have peak emission in the optical¹ and become very faint relative to the disk's emission at longer (hundreds to thousands of microns) wavelengths. Fig 1.2 presents a spectral energy distribution, or SED, showing emission intensity as a function of wavelength from an imaginary disk system.

However, to understand these types of observation, one must first understand the nature of the "telescope" making the observations. What follows is a brief introduction to radio interferometry, followed by a deeper explanation of continuum and line emission.

1.1.1 Interferometry

Interferometry is a clever way to make extremely high-resolution observations at long wavelengths without needing to use incredibly large collecting areas. Were

¹Why, then, is the dust still bright relative to the star? While it's true that the flux *per area* of the dust is significantly smaller than of the star, the dust has a far greater surface area, allowing it to compensate and still be a bright emitter.

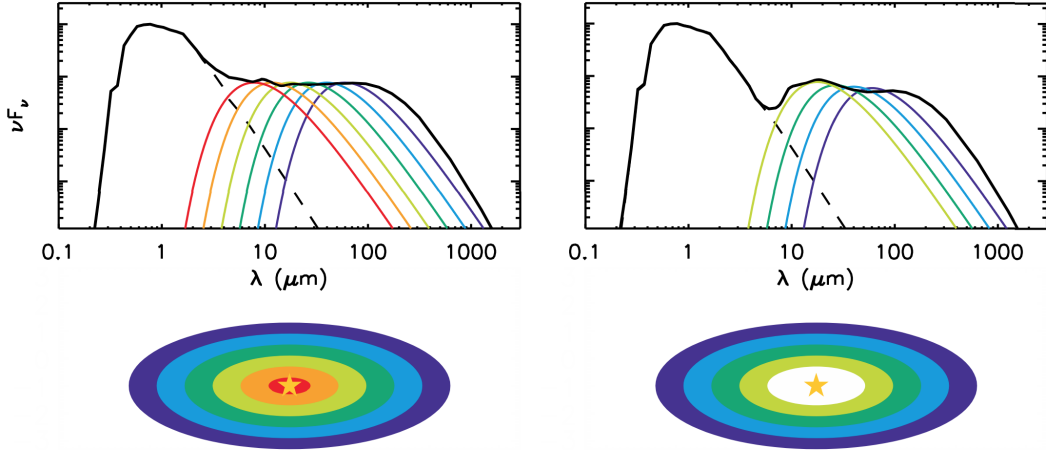


Figure 1.2: Two example SEDs, accompanied by cartoon models to illustrate the various contributions of different elements of a disk and their influences on the SED. The dashed line corresponds to emission from the stellar photosphere, while the colored lines are blackbody curves corresponding to emission from the similarly-colored ring in the cartoon disk below each SED. Curves that peak at shorter wavelengths come from hotter dust. REWORK

one to naively attempt to create a "traditional" (single-aperture) telescope to capture radio emission, they would quickly recall that, for a telescope with a single circular aperture of diameter D , maximum angular resolution is given by

$$\theta \& = 1.22 \frac{\lambda}{D}, \quad (1.1)$$

where θ is the angular resolution achieved, and λ is the wavelength of the emission being observed. Unfortunately, light in the radio regime has wavelengths on the order of millimeters to centimeters, orders of magnitude longer than optical light, which is in the hundreds of nanometers. Consequently, to achieve a resolution comparable to that of an optical telescope, one would have to increase their aperture's diameter accordingly to match the increase in λ . Some have tried this approach: the Arecibo Observatory in Puerto Rico and the Five hundred

meter Aperture Spherical Telescope in China (with diameters of 300m and 500m, respectively) are two immediate examples, but both still have resolutions ($\sim 25''$ for Arecibo and $\sim 15''$ for FAST, observing 3cm emission) that are too coarse to resolve the length-scales that we would like when observing disks. Building and maintaining apertures this big is also an extreme challenge, requiring mountains to be hollowed out, making this an unappealing solution.

The alternative, of course, is to leverage the power of interferometry for a solution to the problem. In an interferometric system, one may reconstruct an image using the interference patterns between light received by two or more separate apertures. In this case, the maximum angular resolution becomes inversely proportional to the maximum distance, or baseline, between any two apertures, which can be made almost arbitrarily large. Interferometry does come with tradeoffs, however, the most notable of which is in sensitivity, since sensitivity is proportional to collecting area and each dish in an interferometer is typically fairly small². Interferometers also intrinsically have spatial filtering, meaning that they are not sensitive to flux from large angular scales. This is because the largest angular scale of a flux source that a telescope is sensitive to is inversely proportional to its smallest baseline. Since the collecting area of a single-dish telescope is a continuous surface, its smallest "baseline" is essentially infinitely small, whereas for an interferometer, that smallest baseline is typically ones to tens of meters. Therefore, interferometers are intrinsically unable to capture flux from sources with angular scales larger than λ/D_{\min} ³.

While this interference process can be done at optical wavelengths with CCDs,

²With ALMA, this is mitigated by the fact that each dish is actually fairly large, at 7 or 12 meters in diameter.

³This can actually be an advantage, however, as it offers the opportunity to choose the length-scale being observed, i.e. remove cloud contamination (large scale structure) from an image of a disk (a small structure).

it is far more difficult to execute, as light must be forced to physically interact before reaching the sensor via a complex and extremely precise optical system. At longer wavelengths, however, heterodyne receivers may be used, making the task of interfering the signals a digital process, rather than a physical one. A heterodyne receiver records both the amplitude (analogous to the intensity that a CCD might measure) and the phase of the signal it receives. Because the receiver captures phase information as well as amplitude, the signals from two dishes may be digitally interfered after being received. Physical features must be calibrated out, including phase delay caused by differences in line-of-sight path length from the source between the receivers, atmospheric effects, and instrumental phase delays. The result, for a single baseline, is a complex voltage pattern describing the amplitude and phase of the interference pattern between the signal each dish received.

The full output from an interferometer is a collection of these signals which, taken together, approximate the Fourier transform of the sky image. We say that this output lives in the "visibility domain", which itself is a Fourier transform of the image domain. The voltage pattern from each baseline is called a visibility, and relates to the full set of visibilities analogously to the relationship between a pixel and an image.

While the image domain has spatial dimensions (i.e. the xy plane), the visibility domain instead uses the uv plane. The uv plane is a wavelength-scaled $x - y$ coordinate system parallel to the sky in the direction of the target source. Here "wavelength-scaled" can be taken to mean that $u = X/\lambda, v = Y/\lambda$, where λ is the wavelength of observation and X and Y are the lengths of the x and y (i.e. north/south, east/west) components of the projected baseline. Thus, each baseline samples a specific spatial frequency, given by $\theta = 1/\sqrt{u^2 + v^2}$. An inter-

ferometer may thus be represented on the uv plane as a scatter of points, where each point corresponding to the wavelength-scaled, target-projected, component distance between two receivers. The ideal aperture would completely fill the uv plane, so that every spatial frequency was sampled. However, since the number of baselines we may access is very limited (approximately the square of the number of antennae in an array), this is clearly an impossibility for an interferometer⁴

However, the fact that the *projected* baseline is really what determines visibility's location in the uv plane, rather than the baseline's "true", un-projected length, allows us to cleverly gain far more points in the uv plane than one might immediately expect. Since the Earth rotates throughout the night, the projection of a given baseline relative to the target source will change throughout the night as well. Consequently, by making observations over the course of a night, many more points in the uv plane may be sampled, thus giving a better-filled plane. This process is known as "Earth rotation aperture synthesis."

We would now like to consider to to recover an image from a set of observed visibilities. In general, moving between frequency space and distance space is given by a simple Fourier transform. When considering this translation for telescopes, we consider the shape of the image produced by observation of a single point source directly on axis with the aperture. For a conventional telescope with a circular aperture, coverage in the uv plane is in the shape of a filled circle of constant amplitude. Translation to the image domain, via a Fourier transform of that shape, results in the familiar 2-D Airy Disk, the characteristic point-spread function (PSF) of a single aperture convolved with a point source. With an interferometer, this process would be equally straightforward if the uv plane

⁴Of course, a single-aperture telescope does not have this problem since its uv plane is one continuous collecting area and thus can be seen as having infinite baselines and complete uv coverage.

were fully sampled, but because it is not, the resulting image is instead a Fourier transform of all the points in the uv plane sampled by the baselines, and can take on a very complex shape⁵. However, while this shape is complex, it is still - just as is the case in the optical - just a convolution of the point source with some PSF, only in this case the PSF is more complicated than an Airy function. As we increase the number of uv points sampled, the resulting image will increasingly approximate a bumpy and/or elongated Airy disk. In radio astronomy, we call this PSF the "dirty beam".

When observing a source, we would like to find the true sky brightness pattern (i.e. the sky image). As described above, the Fourier transform of a set of visibilities is a convolution of the dirty beam with the true sky brightness pattern. Therefore, we would like to remove the dirty beam's contributions to the image. The process of removing the influence of the dirty beam, and the artifacts it can introduce, is called deconvolution. In practice, this deconvolution process takes the form of some iterative algorithm that selectively removes the effects of the dirty beam. The interested reader is directed to the CLEAN algorithm (Hogbom (1974) reference), the first and most popular process (and the one used in this work), as well as the maximum-entropy method (e.g. Wernecke & D'Addario (1977 reference), Skilling & Bryan 1984 reference).

In summary, interferometry works by recording amplitude and phase information about some emission with many radio antennae and digitally interfering each antenna's signal with the signal received by every other telescope. Each of the resulting interference patterns is called a visibility, and represents a point in

⁵ Additionally, thanks to the incomplete sampling of the uv plane, an infinite number of images could all be consistent with some given finite set of visibilities, although many of them would not be physically possible. The one we choose to look at is determined by our deconvolution process, but is not actually the true image.

uv space. Translation from the visibility domain to the image domain involves taking the Fourier transform of the visibilities and deconvolving the dirty beam's influence. Finally, one is left with a clean science image. It is worth noting that the final science product - the data that we ultimately use for analysis - is the visibility set, rather than the translated image, since the imaging process introduces artifacts and does not produce a unique result (described above). This means that the specific parametrization of CLEAN or any other step in the imaging process does not need to be perfect.

Currently, the world's most advanced interferometer, and the source of this thesis's data, is the Atacama Large Millimeter/Submillimeter Array (ALMA), seen in Fig 1.3a. Built in the high Chilean desert at around 5,000 meters (16,000 feet), the \$1.4-billion array first opened its eyes for scientific observation in mid-2011, with funding from a global partnership between Chile, the United States, Europe, and several other countries. With its 66 total antennae (50 12-m dishes and 16 at 7-m) and baselines extending out to 15-km, it offers an order of magnitude increase in sensitivity and resolution over previous arrays that observe at similar frequencies, which include the Submillimeter Array (8 6-meter dishes), NOEMA (10 15-meter dishes) and the CARMA (23 dishes of 3.5-m, 6.1-m, and 10.4-m diameters).

The effects of this increase are striking; gaps and rings in faraway disks are now resolvable in striking clarity (Andrews et al 2018 reference; Fig. 1.3b), providing a treasure-trove of opportunity to hone our understanding of disk evolution and planetary-system formation. ALMA has also been a blessing to other subfields of astronomy as well, enabling high-resolution observations of everything from complex organic molecules in disks (Walsh et al 2019, Podio et al 2019 reference) to gravitational lensing from dark matter halos (Herrera-Martin et al (2019) refer-

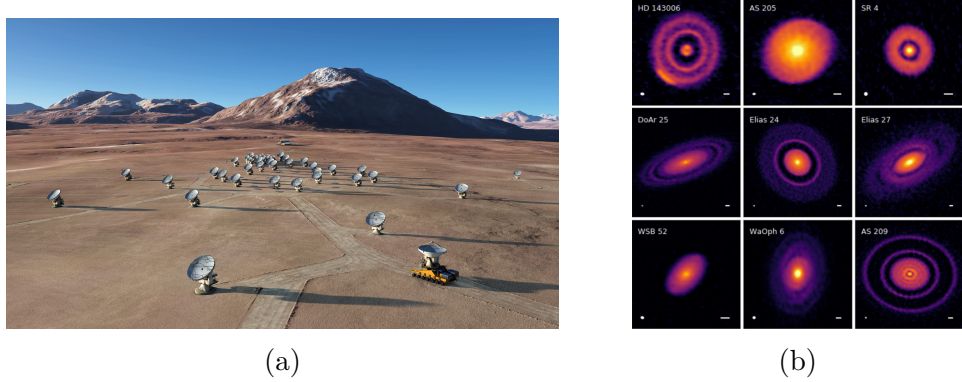


Figure 1.4: Left: A rendering of ALMA (reference) shows the interferometer’s antennae in the high desert, as well as a purpose-built truck moving one of the antennae (lower right). Right: A recent survey from ALMA reveals stunning detail in several protoplanetary disks. Andrews et al 2018 reference

ence) to molecular tori around black holes (Combes et al 2019 reference). These awe-inspiring projects are a small portion of ALMAs contributions to the world of radio astronomy, and more are being made with each passing day.

1.1.2 Continuum Emission

Continuum emission observations integrate flux from a wide band of frequencies, just as our eyes do in the optical. They are appealing for their simplicity and because they are sensitive to faint objects.

When observing protoplanetary disks, an understanding of planet formation is often a guiding motivation. One parameter that is critical to the planet-forming process is total disk mass. We know that, to first order, when a disk is optically thin, its total mass, M_{disk} , is linearly proportional to its flux density, F_ν (reference Hildebrand 1983), found from an observation of continuum emission. This relationship is given by

$$M_{\text{disk}} = \frac{F_\nu d^2}{\kappa_\nu B_\nu(T_c)}, \quad (1.2)$$

where d is the source's distance, κ_ν is an assumed dust opacity, and $B_\nu(T_c)$ is the Planck function at a given characteristic temperature, T_c . The value of T_c and disk opacity can be inferred without much difficulty by fitting the disk's SED using a simple model. This function is, of course, rather approximate; it assumes a single temperature and single dust opacity (a function of composition and grain size distributions) throughout the disk. The assumption of optically thin emission means that calculations made will inherently be lower limits, since any substantial optical depth will block emission from inner regions of the disk. Furthermore, even in the case of optically thin emission, significant mass may be locked up in bodies that are invisible to our observations. Still, it is a useful tool that can be used to approximate disk mass using continuum emission images.

1.1.3 Line Emission

As molecules collide with one another or absorb light, they gain energy, entering higher rotational energy states. However, as their presence in these states cannot be sustained without the addition of more energy, they will de-excite soon after. This de-excitation process - stepping down from one rotational energy state to the one below - causes the emission of light. Every transition in every molecule emits at its own specific frequency, or rest frequency, making that light identifiable to observers. We may observe a specific rotational transition from a single type of molecule by tuning our receiver to be sensitive to a very narrow window of frequencies immediately around the rest frequency of the transition of interest.

The narrow range of frequencies at which a molecule emits makes ALMA's large sensitivity particularly crucial for observations of molecular lines at high spectral resolution or in rare species.

One immediate feature that line emission gives us access to is velocity information: since all emission should have a single frequency (the transition's rest frequency)⁶, we immediately know that any variation from that central frequency is a result of Doppler shifting caused by line-of-sight velocity. This allows us to make a "moment-one" map of emission, which shows the intensity-weighted velocity structure of the disks (Fig 1.5)

Observations of line emission also give us information about both the temperature and density structures of the disk, since these are the two factors that influence how much emission we may observe. However, in optically thin emission, the two are degenerate, since an increase in either one will increase emission intensity. In this case, we may combine observations of multiple species to model the temperature. In the case of an optically thick line, however, the temperature and density are no longer degenerate, since all emission originates from the $\tau = 1$ surface, which removes density from the equation and gives us a value for the temperature at that point in the disk's vertical structure. This is valuable, since the a disk's vertical temperature profile varies significantly, with the surface notably warmer than the midplane.

Besides offering information about radial density and temperature profiles, line emission also provides another way of finding total disk mass. Like the initial cloud that the star and disk formed from, the vast majority of the disk's mass comes in its gas, and like that initial cloud, the vast majority of that gas is molecular

⁶Technically, the uncertainty principle tells us that a line will have some "natural" width, but this width is small compared to the Doppler width

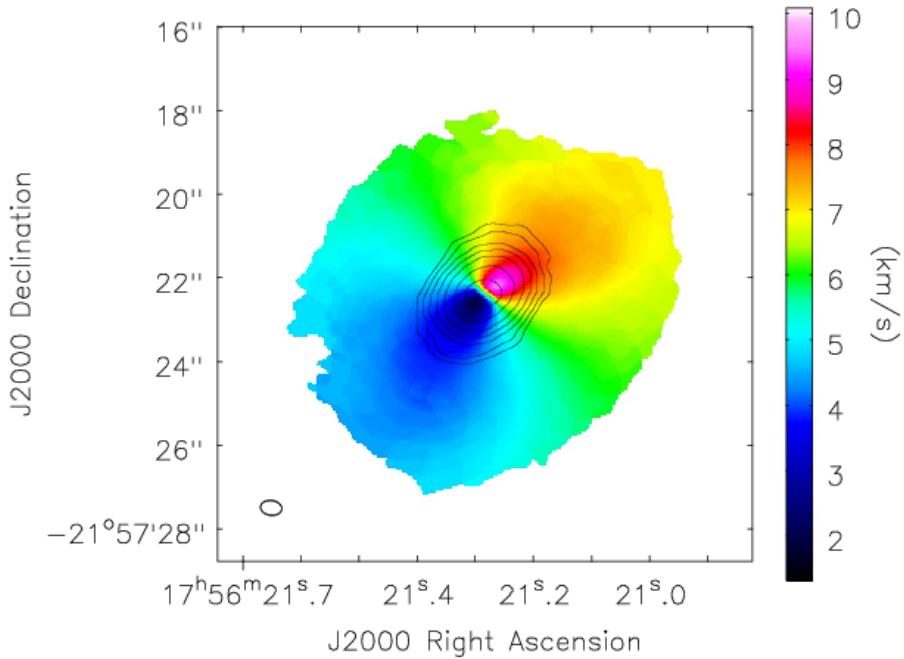


Figure 1.5: An example of a moment-one map of a protoplanetary disk that is seen approximately edge-on, drawn from de Gregorio-Monsalvo et al 2013 reference. Colors correspond to intensity-weighted velocity; in other words, how quickly material is moving relative to the observer. This image immediately offers us several pieces of information: for example, the disk’s northeast side is moving away from us while the southwest side is coming towards us, and the disk as a whole is receding from us at around 6 km/s, which we know due to the fact that the material with zero disk velocity (in green) corresponds to a velocity of 6 km/s relative to us.

hydrogen, or H₂. However, since H₂ is a symmetric molecule and thus has no permanent dipole moment, it has no rotational transitions and does not emit in the radio, making it invisible to our instruments. As a consequence, we must instead observe emission from other molecules, make assumptions about relative abundances of that molecule to H₂, and extrapolate the total disk mass from there.

The second most abundant molecule behind H₂ is CO. Thanks to its abundance, as well as its relatively low excitation temperature, CO provides robust,

bright emission. Drawing on measurements of CO/H₂ ratios in warm dense cloud (e.g. Aikawa & Herbst 1999; Fogel et al. 2011 reference), we use a ratio of 1:10000, or 10⁻⁴, to determine COs relative abundance in protoplanetary disks. Ratios for less prominent molecules with more complicated chemistry (including HCO⁺, HCN, CS, CN, methanol, and others) are drawn from the interstellar-medium literature and chemical modeling. It is not clear that these values are constant either with location or age, but are generally assumed to be.

1.2 Disks & The Role of Environment

Line observations of disks in high-mass star-forming regions (SFRs) are significant for two significant reasons. First, they are new; not until ALMA opened its 66 eyes were we able to have such a direct and high-resolution view of young disks in this environment. Second, since there is significant evidence that most stars in our galaxy - including our own Sun (Gaidos et al 2009, Tachibana et al 2006 reference) - formed out of a high-mass SFR (reference), these constraints will provide useful insights into the general disk evolution process, and contextualize our own system's history. Thus, for both reasons, we would like to better understand the role that environment plays in the development and evolution of protoplanetary disks, comparing them to the well-studied disk population in low-mass (reference) and the one well-characterized disk in a high-mass SFR (Factor et al reference), and evaluate how that environment may affect planet-formation potential.

1.2.1 The Minimum Mass Solar Nebula

The minimum-mass solar nebula (MMSN) is a conceptual aid used to inform astronomers about the distribution of material required to form a planetary system

(MMSN, Weidenschilling 1977). The MMSN is the radial mass profile that our own Solar System would present if the mass of each planet were, rather than being bound up in spheres, instead ground up and spread across the ring bound by the orbits of their inferior and superior neighbors. Gas is then added to the ring until the its gas:dust ratio reaches the canonical interstellar-medium value of 100:1 (meaning that gas giants like Jupiter would have very little gas mass added, while terrestrial planets like Earth would have their mass significantly increased). The resulting mass profile represents the minimum surface density required to form our own protoplanetary disk and thus a way to inform our comparisons of other disks to our own. When this surface density profile is integrated into a single mass, it gives $M_{\text{MMSN}} = 0.01M_{\odot}$.

It is, of course, an extremely approximate characterization. One significant assumption it makes is that our planets formed in their current positions. This is a statement that we know both to be false (Walsh et al. 2011; Tsiganis et al. 2005) and consequential, since planetary migration can cause disks to lose mass by pushing competing planetesimals either out of orbit or into inner regions of the disk where they may be more susceptible to accreting onto the host star.

Another assumption is that the chemistry is radially and temporally constant
REWORK

Still, in spite of this, the MMSN offers us an initial diagnostic tool to determine whether a disk has "planet-formation potential."

1.2.2 Low- and High-Mass Star Forming Regions

Thanks to limitations in sensitivity and resolution, most submillimeter surveys in the pre-ALMA epoch focused on young disks in the nearby low-mass SFRs of

Taurus-Auriga and ρ Ophiuchi. Dust-emission studies of disks in these regions by Andrews & Williams (2005, 2007 reference update with new references) have yielded a wide range of disk masses, with a median of $0.005 M_{\odot}$ and a significant fraction with mass greater than the MMSN. This large fraction of disks with planet-forming potential is consistent with what we would expect based on the enormous - and still growing - number of exoplanets (reference) that have been discovered in the last two decades.

Of course, studying only nearby disks paints an incomplete picture of the population and its evolutionary trends; for one, most stars form in high-mass SFRs (Lada & Lada 2003 reference), and low-mass SFRs are qualitatively different than their high-mass siblings. High-mass SFRs are massive, dense clusters with large abundances of high-mass O and B stars. Protoplanetary disks in these regions experience accelerated mass loss, thanks to the powerful ionizing radiation from the high-mass stars and the increased chance of gravitational interaction caused by their high densities (reference maybe?). This mass loss is likely a problem for planet formation (Johnstone et al. 1998 reference), but its effects are not yet well understood. It is because of these factors that we would like to study disks in high-mass SFRs.

The nearest high-mass SFR to us is the Orion Nebula Cluster (ONC), 389 pc away. The Hubble Space Telescope was the first to dedicate significant time to the ONC, producing an abundance of iconic and awe-inspiring images of the cluster and of the disks it hosts (references). These studies have guided many subsequent observations, including those in the radio. Many of the cluster's protoplanetary disks (or proplyds, as those in the ONC are called) are visibly teardrop-shaped, tailing away from the cluster's biggest, brightest stars. Images like Fig 1.6, showing disks being pushed away from nearby bright stars, and countless others demonstrate



Figure 1.6: NASA press image of a selection of proplyds in the Orion Nebula. The closer a proplyd is to a large, bright star, the more visibly windswept it is. Image courtesy of HST

the harsh environment that these young disks exist in, thanks to their local O and B stars.

Indeed, the influence of these large stars has already been demonstrated, both in their affect on mass-loss rate and mass distribution. Statistically-significant anti-correlations between disk mass and proximity to the ONC's central O star, θ^1 Ori C, have been shown using both data from the SMA (Mann & Williams 2009 reference) and ALMA (Eisner et al 2018 reference, "Josh Eisner doesn't get all the credit here! Definitely cite Rita Mann's ALMA paper first"). Furthermore, observations characterizing mass-loss rates for these proplyds in the Orion Nebula have found rates of $\dot{M} \approx 10^{-7} M_{\odot} \text{ yr}^{-1}$ (Henney & O'Dell (1999) reference), which implies that a typical disk (i.e. one of MMSN-scale, or $\sim 0.01 M_{\odot}$) would be fully

dispersed before giant planets could form (Hubickyj et al. 2005 reference) and before they could reach the inferred age of the disk-hosting stars in the ONC of ≈ 2 Myr (Reggiani et al. 2011; Da Rio et al. 2009 refernce).

Despite all this, not only do we still see disks, but we still see significant planet-forming potential in the Orion Nebula, potential that is comparable to that of other low-mass SFRs. A full 30% of disks surveyed in the ONC have disks with masses greater than or equal to the MMSN (reference - Rita?), falling comfortably between ρ Ophiuchus' 29% and Taurus' 37% (Andrews & Williams (2005, 2007) reference USE RECENT ALMA REFERENCES HERE).

However, since all these surveys are based exclusively on the analysis of dust continuum emission, the comparison is profoundly hamstrung by its reliance on assumptions of gas/dust ratios drawn from the ISM literature. This means that the resulting understanding of the gas masses in these regions is directly proportional to that 100:1 ratio, a value that is almost certainly not correct (reference); the question is how far off it is and how significantly that ratio varies with environment. The consequences of this assumption are significant as well, since a disk's gas mass directly determines its giant planet forming potential both by setting the amount of raw material available to the forming planet as well as by influencing the environment's turbulence profile and planets' migratory patterns within the disk. Furthermore, these continuum surveys cannot reveal these disks' chemistries and the environmental influences that likely affect them, instead simply assuming solar composition. Together, these assumptions regarding both the total gass mass as well as its composition result in a sizeable caveat accompanying any claims we make about the birth and evolution of protoplanetary disks in high-mass SFRs.

Mann et al 2014 reference made the first survey of the Orion propluds as part

of ALMA's Cycle 0 Early Science operation. The survey studied 22 disks in four molecular lines (HCO^+ , HCN, CO, and CS) and $856\mu\text{m}$ continuum, and calculated each disk's dust mass from the continuum emission.

Since then, only one of the disks has had its line data characteristics analyzed. Factor et al 2017 reference performed an analysis of the radial distribution of gas that by modeling emission from the four lines to try to understand the chemical abundance and physical structure of different molecules in the disk. In the study, they found some weird shit REWORK

The disks that are the subject of this thesis are drawn from the same survey.

1.3 d253-1536: A Misaligned Binary System

The subject of this thesis is the system d253-1536, a misaligned binary (Williams et al 2014 reference) of pre-main sequence stars in the M43 region of the Orion Nebula Cluster. Each star in the system has its own disk, henceforth called disk A and disk B (east and west, respectively, in all images of the system).

1.3.1 Local Environment & Features

d253-1536 is located in M43, a nebula adjacent to M42 (the famous Orion Nebula) and part of the Orion Nebula Cluster (ONC). Many previous surveys have studied disks in the Trapezium cluster, a region near M42's brightest star O-star θ^1 Ori C. Mann et al 2014 reference found a statistically significant correlation between disk mass and distance from θ^1 Ori C in a study of 70 proplyds (Fig. 1.8), particularly within 0.03 pc of the star, where there is a lack of disks more massive than $3M_{\text{jup}}$. These disks are also truncated in radial extent, with no disks extending out past 60 AU in this region (Eisner et al 2018 reference).

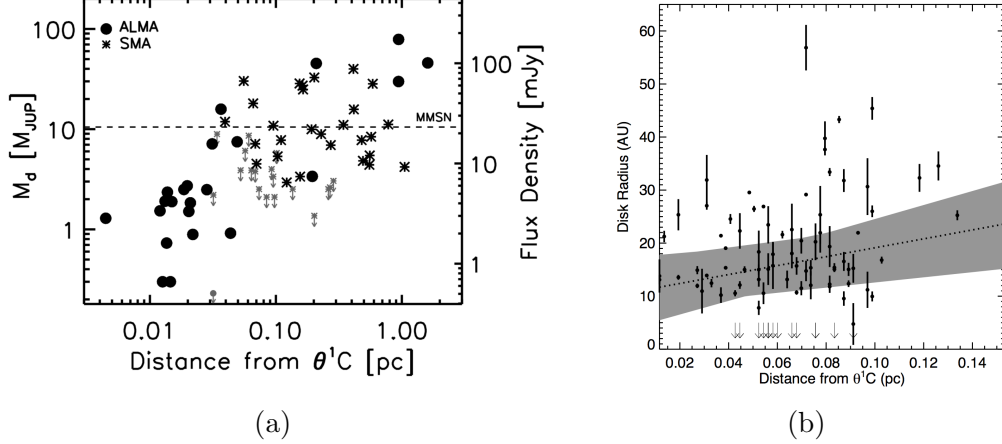


Figure 1.8: *Left:* The masses of 70 ONC proplyds are plotted against their projected distance from the Orion Nebula’s central O-star, θ^1 Ori C, drawn from surveys from ALMA and the SMA (Mann et al 2014 reference). Grey markers indicate 3σ upper limits for non-detections. The dashed line at $10 M_{\text{Jup}}$ indicates the minimum-mass solar nebula. As is clear from this plot, a statistically-significant correlation was found between disk mass and distance from θ^1 Ori C. *Right:* Radius is also affected by proximity to θ^1 Ori C (Eisner et al (2018) reference)

However, because of M43’s separation from the Trapezium cluster (it lies ≥ 1 pc to the cluster’s north), disks in this region do not experience the same levels of photoevaporation. M43 has only one large emitter, Ori, which is a triple-star system whose main component is a B-type star. d253-1536 is wrapped in an ionization bow shock, HH 668 A, about 1

“

to the system’s west and facing towards Nu Ori, but otherwise the system shows no signs of influence from giant stars, whether in photoevaporation or in morphological influences (Mann & Williams (2009) reference).

The system’s larger disk, disk A (the disk on the left in the images), has a large jet emanating from it in observations in the optical made with HST (Smith

et al 2005 reference). However, since the jet is not visible in the radio, we make no attempt to discuss, model or explain it.

1.3.2 Previous Observations

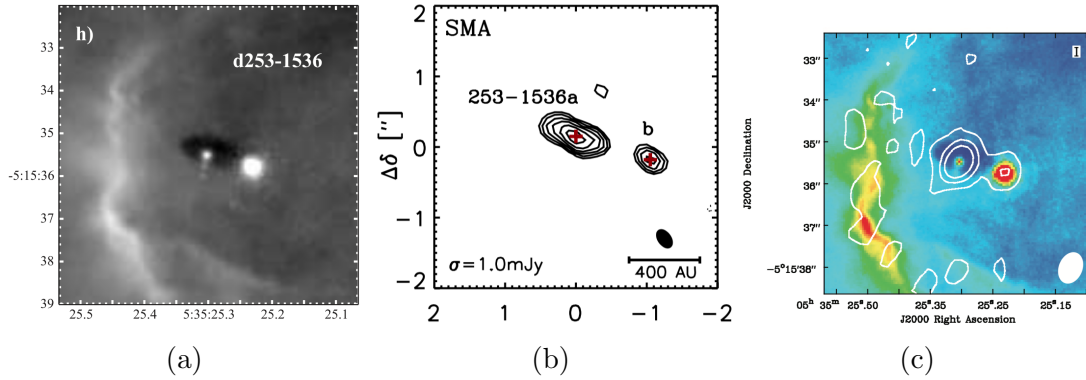


Figure 1.10: Images of V2434 Ori taken from Smith et al (2005 reference) on HST (Fig. 1.9a), Mann et al (2009 reference) with the SMA at $880 \mu\text{m}$ (Fig. 1.9b), and Ricci et al (2011 reference) with the EVLA at 7mm (Fig. 1.9c). The ionization front is clearly visible in both the HST and EVLA observations, and the jet from disk A is visible in the HST image.

First observed by Smith et al (2005 reference) using the Hubble Space Telescope, the authors took interest in what they saw as a binary system containing one star without a disk and one star embedded in a proplyd with a large jet and exhibiting tidal interactions with its companion (Fig 1.9a). Mann & Williams (2009 reference) used $880 \mu\text{m}$ continuum measurements to estimate dust masses of the disks to be $0.066 M_{\odot}$ and $0.018 M_{\odot}$, for disks A and B respectively, making d253-1536a the most massive disk measured in the ONC, significantly larger than the Cluster's second largest disk at $0.034 M_{\odot}$ and adding credence to the theory that θ^1 Ori C is likely responsible for the truncation of disk masses in the Trapezium cluster. Subsequent detections at 7mm by Ricci et al (2011) indicated that both disks are hosts to substantial populations of large dust grains (1.9c),

although the distributions of grain sizes are different in the two disks. The same study also spectral typed the host of d253-1536b to be an M2 star and G2 for d253-1536a's host star.

The system was observed in an ALMA survey of 22 proplyds in M43 by Mann et al (2014 reference) in four molecular lines (HCO^+ (4-3), HCN(4-3), CO(3-2), and CS(7-6); Fig ??), and preliminary fits of the system's kinematics in the HCO^+ (4-3) line were made by Williams et al (2014 reference). Using continuum observations alone and assuming canonical values for temperature, dust opacity, and gas-to-dust ratio, they found disk masses of 0.074 M_\odot and 0.028 M_\odot for disks A and B, respectively, larger than the previous values. They found an inclination for disk A of $i_A \sim 65^\circ$, but did not resolve disk B and thus were unable to determine its inclination. They found systemic LSRK velocities of 10.55 and 10.85 km/s for the two disks, which are close enough to be well within the escape velocity that the authors calculated for a disks at their projected separation of 440 AU of 2.5 km/s, indicating that the binary is bound. This similarity in systemic velocity also indicates that the binary's orbital plane is likely close to face-on.

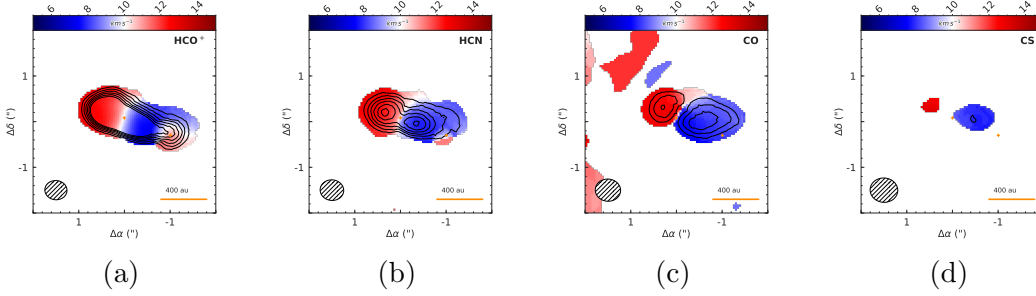


Figure 1.12: Moment-1 maps of HCO^+ , HCN, CO, and CS emission (left to right) in the present study's proplyds.

With our high resolution observations of gas line emission, we aim to determine the temperature, density, and chemical profiles of the system, as well as refining

the mass estimates for both disks and host stars. With this information in hand, we will examine this disk’s characteristics in the context of previously studied disks in the Taurus and Ophiuchus star forming regions, as well as comparing it to the disk studied by Factor et al (2017 reference), and evaluate the disks’ planet forming potentials.

1.4 Summary of Contents

In this work we characterize ALMA observations of two young protoplanetary disks in the d256-1536 system. Observations and data reduction are described in §2. In §3, data and basic analysis are presented. Descriptions of modeling and fitting techniques are discussed in §4, and in §5, best-fit parameters are discussed and contextualized, as well as unexpected features maybe.

Bibliography

- Collaboration, G. 2016, *Astronomy & Astrophysics*, 595, A1, arXiv: 1609.04153
- Collaboration, G., Brown, A. G. A., Vallenari, A., Prusti, T., de Bruijne, J. H. J., Babusiaux, C., & Bailer-Jones, C. A. L. 2018, *Astronomy & Astrophysics*, 616, A1, arXiv: 1804.09365
- Factor, S. M., et al. 2017, *The Astronomical Journal*, 153, 233, arXiv: 1704.01970
- Goodman, J., & Weare, J. 2010, *Communications in Applied Mathematics and Computational Science*, 5, 65
- Mann, R. K., et al. 2014, *The Astrophysical Journal*, 784, 82, arXiv: 1403.2026
- Mann, R. K., & Williams, J. P. 2009, *The Astrophysical Journal*, 699, L55
- Ricci, L., Robberto, M., & Soderblom, D. R. 2008, *The Astronomical Journal*, 136, 2136
- Ricci, L., Testi, L., Williams, J. P., Mann, R. K., & Birnstiel, T. 2011, *The Astrophysical Journal*, 739, L8
- RJ Sault, MCH Wright, R. S. H. P. J. H. P. T. 1995, *ASP Conf. Ser.*, 77, 433
- Sault, R. J., Teuben, P. J., & Wright, M. C. H. 2006, arXiv:astro-ph/0612759, arXiv: astro-ph/0612759
- Smith, N., Bally, J., Licht, D., & Walawender, J. 2005, *The Astronomical Journal*, 129, 382
- Williams, J. P., et al. 2014, *The Astrophysical Journal*, 796, 120, arXiv: 1410.3570